TECHNISCHE UNIVERSITÄT
KAISERSLAUTERN

SCHRIFTEN ZUR

FUNKTIONALANALYSIS UND GEOMATHEMATIK

M. J. Fengler, W. Freeden, A. Kohlhaas,
V. Michel, T. Peters

Wavelet Modelling of Regional and Temporal Variations of the Earth's Gravitational Potential Observed by GRACE

Bericht 21 – Mai 2005

FACHBEREICH MATHEMATIK

Journal of Geodesy manuscript No.
(will be inserted by the editor)

M. J. Fengler · W. Freeden · A. Kohlhaas · V. Michel · T. Peters

Wavelet Modelling of Regional and Temporal Variations of the Earth's Gravitational Potential Observed by GRACE

Received: date / Accepted: date

Abstract This work is dedicated to the wavelet modelling of regional and temporal variations of the Earth's gravitational potential observed by GRACE. In the first part, all required mathematical tools and methods involving spherical wavelets are introduced. Then we apply our method to monthly GRACE gravity fields. A strong seasonal signal can be identified, which is restricted to areas, where large-scale redistributions of continental water mass are expected. This assumption is analyzed and verified by comparing the time series of regionally obtained wavelet coefficients of the gravitational signal originated from hydrology models and the gravitational potential observed by GRACE. The results are in good agreement to previous studies and illustrate that wavelets are an appropriate tool to investigate regional time-variable effects in the gravitational field.

Keywords Spherical Wavelets · GRACE · Gravitational Field · Hydrological Gravity Variations

1 Motivation

Over the last decade wavelets have found important applications in numerous areas of mathematics, physics, engineering and computer science. Wavelets form versatile tools for representing general functions or data sets. They especially become more and more important in Earth sciences since most recent satellite missions deliver millions of data scattered around the globe. Meanwhile spherical wavelets introduced by Freeden and Schreiner (1995); Freeden and Windheuser (1996); Freeden et al. (1998); Freeden (1999) and further developments of them play an important role in the analysis of regional, high-frequent phenomena observed in geophysical, geodetic, magnetic and meteorological applications (see, e.g., Freeden (1999); Freeden and Michel (2004); Fengler et al. (2004a,b); Fengler (2005); Maier (2003); Mayer (2003) and many references therein).

The spherical wavelets discussed here are based on expansions in Legendre polynomials. Hence, they form radial basis functions on the sphere whose argument depends only on the spherical distance between the center of the wavelet and its evaluation point. Therefore, they are an appropriate tool to filter regional signals. We want to highlight this by applying wavelets to regional mass variations observed by the NASA/DLR satellite mission GRACE (Tapley et al. 2004a).

The twin GRACE satellites have been in orbit for more than 3 years. A number of recent studies showed that GRACE is capable of measuring large-scale mass redistributions within the Earth system (e.g. Wahr et al. (2004); Tapley et al. (2004b); Andersen and Hinderer (2005); Rowlands et al. (2005); Han et al. (2005a)). Most of the measured gravitational variations are believed to belong to hydrological mass redistributions, since other effects are corrected for (see Bettadpur (2003)). Consequently, nearly all studies of temporal variations in the gravitational field from GRACE are focusing on the relationship between gravitational variations derived from hydrology models and the GRACE observations.

Hydrological mass redistributions are restricted to the continents. Hydrology models have a poor performance in some areas due to the lack of observations, especially in the polar regions. Thus, if represented in spherical harmonics, the erroneous information is smeared out over the entire globe. Several approaches have been used to overcome this problem: Wahr et al. (1998); Tapley et al. (2004b); Ramillien et al. (2004); Andersen and Hinderer (2005) use a smoothing Gaussian filter proposed by Jekeli (1981), while Wahr et al. (2004) use special averaging kernels tailored to drainage basins and considering satellite errors and leakage errors (Swenson and Wahr 2002; Swenson et al. 2003). Recently, Rowlands et al. (2005) and Han et al. (2005a,b) developed promising new techniques of gravity computation directly

M. J. Fengler, W. Freeden, A. Kohlhaas, V. Michel
University of Kaiserslautern, Department of Mathematics, Geomathematics Group, Tel.: +49-631-205-3867, Fax: +49-631-205-4736
E-mail: freeden@mathematik.uni-kl.de

T. Peters
Technische Universität München, Institut für Astronomische und Physikalische Geodäsie (IAPG)

from the observed inter-satellite distances without using spherical harmonics. The intention of our work is to avoid the problems related to the global character of the spherical harmonics by applying mathematically more appropriate wavelets for the analysis of the regional mass variations observed by GRACE.

2 Preliminaries

In the following we adopt the notation from Freeden et al. (1998). The letters $\mathbb{N}, \mathbb{N}_0$, and $\mathbb{R}$ denote the sets of positive integers, non-negative integers and real numbers. We write x, y to represent the elements of the three-dimensional Euclidean space $\mathbb{R}^3$ endowed with the Euclidean canonical basis $\{\varepsilon^1, \varepsilon^2, \varepsilon^3\}$. Then $x \cdot y = \sum_{i=1}^{3} x_i y_i$ is referred to as the canonical inner product. The corresponding norm is given by $|x| = \sqrt{x \cdot x}$. The unit sphere is represented by Ω, elements of it usually by ξ or η. Consequently, we denote by Ω_R the sphere of radius R, and its interior ball by Ω_R^{int}. As customary the space of all real, square-integrable functions F on Ω is called $L^2(\Omega)$. $L^2(\Omega)$ is a Hilbert space with the inner product given by

$$\langle F, G \rangle_{L^2(\Omega)} = \int_\Omega F(\xi) G(\xi)\, dS(\xi), \qquad F, G \in L^2(\Omega),$$

and the associated norm

$$\|F\|_{L^2(\Omega)} = \left(\int_\Omega F^2(\xi)\, dS(\xi) \right)^{1/2}, \qquad F \in L^2(\Omega).$$

As well-known the real-valued spherical harmonics $Y_{n,k}$ of degree n and order k form an orthonormal basis of $L^2(\Omega)$ (see, for example, Edmonds (1964); Freeden et al. (1998)). Hence each $F \in L^2(\Omega)$ can be written uniquely in $L^2(\Omega)$-sense in terms of a Fourier series, i.e.,

$$F = \sum_{n=0}^{\infty} \sum_{k=-n}^{n} F_{n,k} Y_{n,k},$$

with

$$F_{n,k} = \int_\Omega F(\eta) Y_{n,k}(\eta)\, dS(\eta).$$

As another important ingredient we require the Legendre polynomials $t \mapsto P_n(t)$ of degree n which are, for instance, obtainable via the Rodriguez formula

$$P_n(t) = \frac{1}{2^n n!} \frac{d^n}{dt^n} (t^2 - 1)^n, \qquad t \in [-1, 1].$$

Altogether, we end up at the spherical addition theorem

$$\sum_{k=-n}^{n} Y_{n,k}(\xi) Y_{n,k}(\eta) = \frac{2n+1}{4\pi} P_n(\xi \cdot \eta)$$

connecting the spherical harmonics and the Legendre polynomials (see Freeden et al. (1998)). As a matter of fact, the latter equation forms the foundation in formulating scaling functions and wavelets on the sphere.

2.1 Scaling Functions and Wavelets

First, we require a so-called generator of a scaling function. The choice of this generator determines all properties of the spherical function and its associated wavelet:

A family $\{\{\Phi_J^\wedge(n)\}_{n \in \mathbb{N}_0}\}_{J \in \mathbb{N}_0}$ is called a generator of a scaling function, if it satisfies the following requirements:

1. For all $J \in \mathbb{N}_0$
$$(\Phi_J^\wedge(0))^2 = 1, \tag{1}$$
2. for all $J, J' \in \mathbb{N}_0$ with $J \le J'$ and all $n \in \mathbb{N}$
$$0 \le (\Phi_J^\wedge(n))^2 \le (\Phi_{J'}^\wedge(n))^2, \tag{2}$$
3. for all $n \in \mathbb{N}$
$$\lim_{J \to \infty} (\Phi_J^\wedge(n))^2 = 1. \tag{3}$$

For fixed $J \in \mathbb{N}_0$ the sequence $\{\Phi_J^\wedge(n)\}_{n \in \mathbb{N}_0}$ is called the *symbol* of the corresponding scaling function Φ_J of scale J. According to Freeden et al. (1998) this scaling function of scale J is defined by

$$\Phi_J(\xi, \eta) = \sum_{n=0}^{\infty} \Phi_J^\wedge(n) \frac{2n+1}{4\pi} P_n(\xi \cdot \eta). \tag{4}$$

Now, suppose that $\{\{\Phi_J^\wedge(n)\}_{n \in \mathbb{N}_0}\}_{J \in \mathbb{N}_0}$ is a generator of a scaling function. Then the families $\{\{\Psi_J^\wedge(n)\}_{n \in \mathbb{N}_0}\}_{J \in \mathbb{N}_0}$ and $\{\{\tilde{\Psi}_J^\wedge(n)\}_{n \in \mathbb{N}_0}\}_{J \in \mathbb{N}_0}$ are said to be the generators of the primal and the dual wavelet, respectively, if the *refinement equation*

$$\tilde{\Psi}_J^\wedge(n) \Psi_J^\wedge(n) = (\Phi_{J+1}^\wedge(n))^2 - (\Phi_J^\wedge(n))^2 \tag{5}$$

is satisfied for all $J \in \mathbb{N}_0$ and $n \in \mathbb{N}_0$. Consequently, the primal and dual wavelet of scale J, respectively, read as follows:

$$\Psi_J(\xi, \eta) = \sum_{n=0}^{\infty} \Psi_J^\wedge(n) \frac{2n+1}{4\pi} P_n(\xi \cdot \eta),$$
$$\tilde{\Psi}_J(\xi, \eta) = \sum_{n=0}^{\infty} \tilde{\Psi}_J^\wedge(n) \frac{2n+1}{4\pi} P_n(\xi \cdot \eta).$$

Since we consider only P-scale wavelets (see Freeden (1999)) in this work we simply let $\tilde{\Psi}_J(n) = \Psi_J(n), J \in \mathbb{N}_0, n \in \mathbb{N}$. Hence, the symbol is computed by

$$\Psi_J^\wedge(n) = \sqrt{(\Phi_{J+1}^\wedge(n))^2 - (\Phi_J^\wedge(n))^2}.$$

If for all scales J the symbol $\{\Phi_J^\wedge(n)\}_{n \in \mathbb{N}_0}$, respectively $\{\Psi_J^\wedge(n)\}_{n \in \mathbb{N}_0}$, is different from zero only for finitely many values of n, the corresponding scaling function $\{\Phi_J\}_{J \in \mathbb{N}_0}$ and the wavelet $\{\Psi_J\}_{J \in \mathbb{N}_0}$, is called *bandlimited*. For an overview on different types of scaling functions and wavelets we refer to Freeden (1999) and Freeden et al. (1998). In this work we restrict ourselves to the consideration of scaling

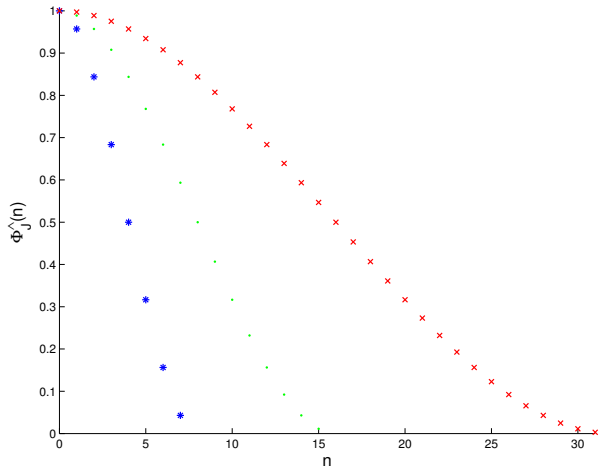

Fig. 1 Symbol of the CuP scaling functions Φ_3, Φ_4, and Φ_5.

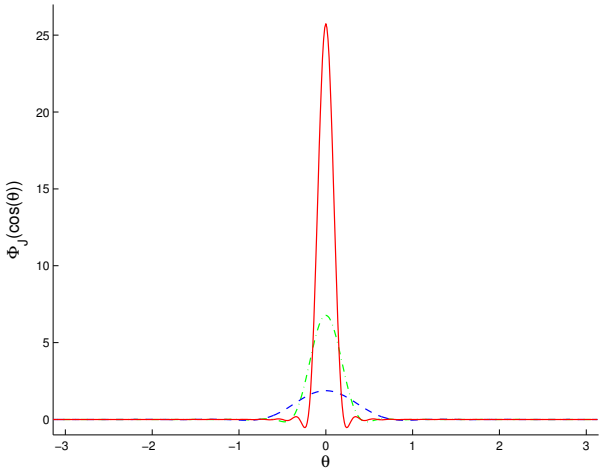

Fig. 2 Sectional plot of the CuP scaling functions Φ_3, Φ_4, and Φ_5.

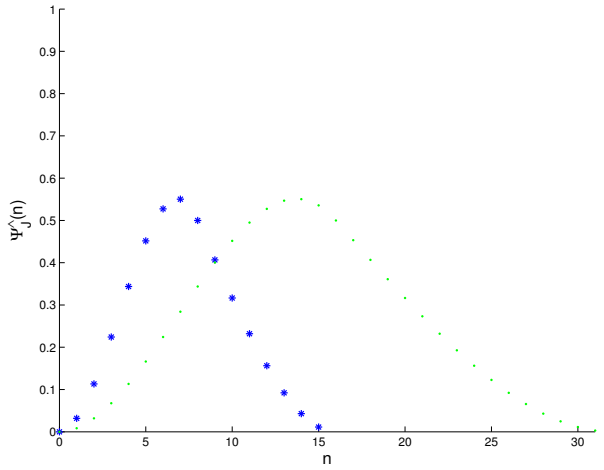

Fig. 3 Symbol of the CuP wavelets Ψ_3, and Ψ_4.

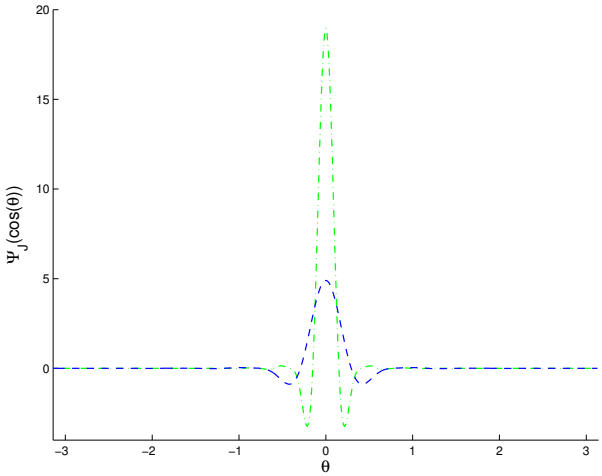

Fig. 4 Sectional plot of the CuP wavelets Ψ_3 and Ψ_4.

functions and wavelets generated by a so called cubic polynomial (CuP) in frequency domain, i.e., we let

$$\Phi_J^\wedge(n) = \begin{cases} (1-2^{-J}n)^2(1+2^{-J+1}n) & \text{for } n \in [0,2^J), \\ 0 & \text{for } n \in [2^J,\infty), \end{cases}$$

from which one can easily verify that all three conditions of a generator are fulfilled. However, it should be remarked that every other generator satisfying (1)-(3) can also be taken into account. Finally, we should outline that the CuP scaling function and wavelets are bandlimited, and possess a well localizing shape in space domain, see Fig. 2 and Fig. 4. The corresponding symbols of the scaling function and the wavelet are shown in Fig. 1 and 3.

Twice convolution between a function $F \in L^2(\Omega)$ and a scaling function $\Phi_J(\eta,\cdot)$ yields the scale approximation $S_J(F)$ of scale J. More explicitly, we have

$$\begin{aligned} S_J(F) &= \Phi_J * \Phi_J * F \\ &= \int_\Omega \int_\Omega \Phi_J(\eta,\cdot)\Phi_J(\eta,\xi)V(\xi)\, dS(\xi)\, dS(\eta). \end{aligned}$$

The latter leads us immediately to the scale space

$$\mathscr{V}_J = \left\{ \Phi_J * \Phi_J * F \,\middle|\, F \in L^2(\Omega) \right\}.$$

In this context, the operator

$$W_J(F) = \tilde{\Psi}_J * \Psi_J * F$$

yields the wavelet approximation of F at scale J and the detail space

$$\mathscr{W}_J = \left\{ \tilde{\Psi}_J * \Psi_J * F \,\middle|\, F \in L^2(\Omega) \right\}.$$

Whereas S_J acts as a low-pass filter we can understand W_J as a band-pass filter. By construction, we obtain a multiresolution analysis satisfying

$$\mathcal{V}_0 \subset \cdots \subset \mathcal{V}_J \subset \mathcal{V}_{J+1} \subset \cdots \subset L^2(\Omega),$$

and

$$L^2(\Omega) = \overline{\bigcup_{J=0}^{\infty} \mathcal{V}_J}^{\|\cdot\|_{L^2(\Omega)}}.$$

Clearly, we can understand the convolution $(\Psi_J * F)(\eta)$ as a *decomposition* of F which provides us with *wavelet coefficients* of scale J at some location $\eta \in \Omega$. Vice versa, we can interpret $\tilde{\Psi}_J * (\Psi_J * F)$ as a reconstruction of F from its wavelet coefficients. This is why we refer in the following to the *decomposition wavelet* Ψ_J and the *reconstruction wavelet* $\tilde{\Psi}_J$.

2.2 Wavelet Variances

Once being equipped with the wavelet coefficients of $F \in L^2(\Omega)$ one can derive a decomposition of the energy $\|F\|^2_{L^2(\Omega)}$ of a signal F in analogy to the well-known approach involving degree variances. To demonstrate the relation between both we let

$$\mathrm{Var}_{n,k}(F) = F_{n,k}^2 = \left(\int_\Omega Y_{n,k}(\xi) F(\xi) dS(\xi) \right)^2,$$

such that

$$\mathrm{Var}_n(F) = \sum_{k=-n}^{n} \mathrm{Var}_{n,k}(F)$$

denote the degree variances. Mathematically spoken, the degree variances are a decomposition of the $L^2(\Omega)$-norm of F, i.e., we arrive at

$$\|F\|^2_{L^2(\Omega)} = \sum_{n=0}^{\infty} \mathrm{Var}_n(F).$$

In case of wavelet variances, we substitute the spherical harmonics by our localizing basis functions. In detail, the dimensionless wavelet variances of scale $J \in \mathbb{N}_0$ and location η are given by

$$\begin{aligned} \mathrm{Var}_{J;\eta}(F) &= \left(\int_\Omega \Psi_J(\xi,\eta) F(\xi) dS(\xi) \right)^2 \\ &= ((\Psi_J * F)(\eta))^2, \end{aligned} \tag{6}$$

where $\eta \in \Omega$. Hence, we can interpret (6) as the regional energy content in the signal F located around $\eta \in \Omega$. To make this more evident, we let $\Psi_{-1} = \Phi_0$ and borrow from Freeden and Michel (2004) that

$$\|F\|^2_{L^2(\Omega)} = \sum_{J=-1}^{\infty} \int_\Omega \mathrm{Var}_{J;\eta}(F)\, dS(\eta).$$

Due to their strong relation to a regional energy content of a signal, the wavelet variances provide an appropriate tool for a wavelet compression of the gravitational field data. Moreover, they can be used for (spatial) denoising procedures as proposed by Freeden and Maier (2002).

3 GRACE and Hydrology Data

The GRACE science team released over 20 monthly gravitational fields in terms of spherical harmonic coefficients. They are–besides some gaps–nearly continuous in time. We use 22 fields between April/May 2002 and July 2004. The coefficients are given up to harmonic degree and order 120 except for January 2004 (up to 70) together with so-called "calibrated" error files. According to Tapley et al. (2004b), terms of degree zero, one and two were omitted, since they show a special behavior (see Chen et al. (2004)).

In order to avoid aliasing effects of the high-frequent mass variations of tides and the atmospheric and oceanic circulation, their influence is already removed during the data processing using models (see Bettadpur (2003)). Under the assumption of error-free de-aliasing models, most of the remaining monthly gravity anomalies are generated by hydrological mass redistributions.

Hydrological mass variations are the sum of water redistributions on the continents involving precipitation, evaporation, surface runoff, snow coverage, soil moisture and groundwater storage. There are different global models of these processes available. For this study we used the Climate Prediction Center (CPC) model (Fan and vd Dool (2004)) and the Land Dynamics (LaD) model (Milly and Shmakin (2002)) in their current versions. While the CPC model covers the whole considered time span, the LaD (release "LaD-World-Danube") model stops in April 2004.

4 Application to GRACE Models.

In case of GRACE the gravitational potential V^{GRACE} is provided via dimensionless Fourier coefficients $\tilde{V}_{n,k}$ corresponding to fully-normalized spherical harmonics. These spherical harmonics differ by a factor of $1/\sqrt{4\pi}$ to those introduced above. Exploiting this expansion one obtains a representation of V in $\mathcal{V}_J$ by

$$\begin{aligned} S_J\left(V^{\mathrm{GRACE}}\right)(t,x) &= \left(\Phi_J * \Phi_J * V^{\mathrm{GRACE}}\right)(t,x) \\ &= \sqrt{4\pi}\frac{GM}{R} \sum_{n=3}^{120} \sum_{k=-n}^{n} \tilde{V}_{n,k}(t) \\ &\qquad \times (\Phi_J^\wedge(n))^2 Y_{n,k}\left(\frac{x}{|x|}\right), \end{aligned}$$

where $x \in \Omega_R$, respectively, in the wavelet space $\mathscr{W}_J$ by

$$W_J\left(V^{\mathrm{GRACE}}\right)(t,x) = \sqrt{4\pi}\frac{GM}{R}\sum_{n=3}^{120}\sum_{k=-n}^{n}\tilde{V}_{n,k}(t) \times (\Psi_J^{\wedge}(n))^2 Y_{n,k}\left(\frac{x}{|x|}\right).$$

The latter representation provides us with the dimensionless wavelet coefficient at some location $y \in \Omega_R$, i.e.,

$$\frac{R}{GM}\left(\Psi_J * V^{\mathrm{GRACE}}\right)(t,x) = \sqrt{4\pi}\sum_{n=3}^{120}\sum_{k=-n}^{n}\tilde{V}_{n,k}(t) \times \Psi_J^{\wedge}(n) Y_{n,k}\left(\frac{x}{|x|}\right). \tag{7}$$

A time series of wavelet coefficients computed by (7) is illustrated in Fig. 17 and Fig. 18.
For our study of the temporal variations we subtract an annual mean potential V_{mean} of the fields computed from the months August 2003 - July 2004 (except for January 2004).

5 Application to Hydrology Models

We compute the gravity variations ΔV^{Hyd} from surface density variations $\Delta\rho$ provided by the LaD model and from water column heights provided by the CPC model. Since the gravity variations discussed here are induced by variations in density, we are concerned with $\Delta\rho(t,\cdot)$ which is of class $L^2(\Omega_R^{\mathrm{int}})$ for all times t. Then

$$\Delta V^{\mathrm{Hyd}}(t,x) = G\int_{\Omega_R^{\mathrm{int}}}\frac{\Delta\rho(t,y)}{|x-y|}\,dV(y), \qquad x \in \Omega_R^{\mathrm{ext}}. \tag{8}$$

We borrow from Freeden et al. (1998) that

$$\frac{1}{|x-y|} = \frac{1}{|x|}\sum_{n=0}^{\infty}\left(\frac{|y|}{|x|}\right)^n P_n\left(\frac{x}{|x|}\cdot\frac{y}{|y|}\right). \tag{9}$$

Inserting (9) into (8) and interchanging the summation and integration we deduce

$$\Delta V^{\mathrm{Hyd}}(t,x) = \frac{G}{R}\sum_{n=0}^{\infty}\int_{\Omega_R^{\mathrm{int}}}\left(\frac{|y|}{R}\right)^n \Delta\rho(t,Ry) \times P_n\left(\frac{x}{|x|}\cdot\frac{y}{|y|}\right)\,dV(y),$$

for $x \in \Omega_R$.
Following Wahr et al. (1998) we assume that the density variations occur only in a thin layer of thickness $H \ll R$ close to the surface Ω_R. Then

$$\begin{aligned}\Delta V^{\mathrm{Hyd}}(t,x) &\approx \frac{GR^2}{R}\sum_{n=0}^{\infty}\int_{\Omega}\Delta\rho(t,Ry)P_n\left(\frac{x}{|x|}\cdot\frac{y}{|y|}\right)\,dS(y) \times \underbrace{\int_{R-H}^{R}\left(\frac{r}{R}\right)^{n+2}dr}_{\approx H} \\ &\approx GR\sum_{n=0}^{\infty}\int_{\Omega}\Delta\rho(t,Ry)HP_n\left(\frac{x}{|x|}\cdot\frac{y}{|y|}\right)\,dS(y),\end{aligned}$$

for $x \in \Omega_R$.
Now, we introduce the quantity $\Delta\sigma(t,Ry) = \Delta\rho(t,Ry)H$, which can be understood as a surface density [kg/m^2]. Extending the right hand side by the Earth's mass $M = \frac{4\pi R^3}{3}\overline{\rho}$ we derive

$$\Delta V^{\mathrm{Hyd}}(t,x) = \frac{GM}{R}\sum_{n=0}^{\infty}\int_{\Omega}\frac{3}{4\pi\overline{\rho}R}\Delta\sigma(t,y) \times P_n\left(\frac{x}{|x|}\cdot\frac{y}{|y|}\right)\,dS(y),$$

for $x \in \Omega_R$. By assumption we have $\rho(t,\cdot) \in L^2(\Omega_R^{\mathrm{int}}) \subset L^1(\Omega_R^{\mathrm{int}})$ for all $t \in \mathbb{R}$. Thus, we are allowed to interchange integration and summation in the following. Similar to the J-level approximation of the gravitational field we arrive at

$$S_J\left(\Delta V^{\mathrm{Hyd}}\right)(t,x) = \frac{GM}{R}\int_{\Omega}\sum_{n=0}^{\infty}\frac{3}{4\pi\overline{\rho}R}(\Phi_J^{\wedge}(n))^2\Delta\sigma(t,Ry) \times P_n\left(\frac{x}{|x|}\cdot\frac{y}{|y|}\right)\,dS(y),$$

for $x \in \Omega_R$. We deal with mass variations on the Earth's surface, so we have to consider loading by taking the Love numbers into account. This leads us to

$$S_J\left(\Delta V^{\mathrm{Hyd}}\right)(t,x) = \frac{GM}{R}\int_{\Omega}\sum_{n=0}^{\infty}\frac{3(1+k_n')}{4\pi\overline{\rho}R}(\Phi_J^{\wedge}(n))^2 \times \Delta\sigma(t,Ry)P_n\left(\frac{x}{|x|}\cdot\frac{y}{|y|}\right)\,dS(y),$$

where k_n' denotes the load Love number. We use the values from Wahr et al. (1998). Hence, we can rewrite the latter equation in terms of spherical convolutions by

$$S_J\left(\Delta V^{\mathrm{Hyd}}\right)(t,\cdot) = \frac{GM}{R}\Phi_J * \frac{3}{\overline{\rho}R}\Phi_J^{\mathrm{L}} * \Delta\sigma(t,R\cdot),$$

where Φ_J^{L} denotes the modified scaling function

$$\Phi_J^{\mathrm{L}}(\xi,\eta) = \sum_{n=0}^{\infty}\Phi_J^{\wedge}(n)\frac{1+k_n'}{4\pi}P_n(\xi,\cdot\eta), \qquad \xi,\eta \in \Omega.$$

The superscript L denotes its association to the Love numbers. The reconstruction scaling function Φ_J is as defined as

in (4). Analogously, we derive the representation in terms of spherical wavelets. Then

$$W_J\left(\Delta V^{\mathrm{Hyd}}\right)(t,\cdot) = \frac{GM}{R}\tilde{\Psi}_J * \frac{3}{\bar{\rho}R}\Psi_J^{\mathrm{L}} * \Delta\sigma(t,R\cdot).$$

The wavelet decomposition $\Psi_J^{\mathrm{L}} * \Delta\sigma$ is computed numerically since the data describing the surface density as well as the moisture are only given on the continents. For the numerical integration we choose a polynomially exact integrating, equi-angular grid as proposed, e.g., by Driscoll and Healy (1994).

6 Numerical Results

Since the GRACE observations are known to be dominated by large seasonal continental mass variations, we give results for these phenomena using the method described above. The extrema of the variations occur in spring and autumn. The Fig. 5, 6, and 11, 12 show the variation of the gravitational potential from GRACE relative to the mean in October 2003 and April 2004, respectively. The wavelet scales 3 and 4 are given. Roughly speaking, these scales correspond to the spherical harmonic degrees 8-15 and 16-31 (see Fig. 3). Higher scales are not representative due to the increase of the GRACE errors with increasing degree (Wahr et al. 2004; Tapley et al. 2004b). At lower wavelet scales (e.g., 2 or less which are not shown here) the wavelets take a large area into account (half of the globe or more). Consequently, these scales mix up oceanic with continental areas or even polar with equatorial regions. This is unfavorable when considering regional gravity variations. The influence of the farther distant surrounding decreases massively when considering higher frequent regional signals as it is shown in Fig. 5-16. The largest variations show up for the well-known large drainage basins like the Amazon, the Congo, the Zambezi or the watershed of the Bay of Bengal (Ganges).

The Fig. 7, 8, 13, 14, and 9, 10, 15, 16 display the same quantities as in case of GRACE for the LaD and the CPC model. The differences between the models and the differences relative to the GRACE observations are due to inaccuracies in both, the GRACE observations and the hydrology models. In detail, the GRACE observations still contain non-modelled effects such as other remaining or neglected mass redistributions, e.g. from ocean tides, in the atmosphere or from ice melting and post-glacial rebound. On the other hand, the deviations with and between the hydrology models can be due to irregularly distributed, inhomogeneous and sometimes maybe erroneous input data as well as mathematical approximations of physical processes. Therefore, we cannot expect a perfect agreement. For example, while the LaD model results in smaller amplitudes in general, the CPC model seems to underestimate the variations in the polar regions associated with accumulation and melting of snow. However, when focussing at typical drainage basins, a quite good agreement can be observed, which will be discussed below. For a closer look at the temporal evolution of the global variations, we refer to the electronic supplement.

A restriction to selected drainage basins can easily be obtained by looking at the time series of the wavelet coefficients. The Fig. 17 and 18 give examples for the wavelet scales 3 and 4. The names of the cities Memphis (USA/Tennessee), Manaus (Brazil) and Monghyr (India) are used on behalf of the areas of the Mississippi, the Amazon and the watershed of the Bay of Bengal. In Manaus and Monghyr a seasonal signal is clearly dominant, while Memphis shows also some other effect. The Mississippi area has a minor signal, which might be on the limit of detectability for GRACE. It is interesting, that none of the three curves can be described by a simple sine. The time series also reveals a delay of the maximum of the signal between the GRACE data and the hydrology model prediction of approximately one month, which was already mentioned by Wahr et al. (2004).

The agreement between the GRACE observations and the hydrology models is very impressive. This is evident, when looking at correlation coefficients between the time series illustrated in Fig. 17 and 18. In particular, we obtain in Table 1-3 that the GRACE signal is highly correlated to the hydrology signal. Again, the CPC model performs best in the Bay of Bengal. Also the Amazon basin yields high correlations for both models, while the Mississippi is worse. Still, the numbers are excellent when comparing to the spatial coefficients computed by Andersen and Hinderer (2005) for inter-annual gravity variations.

Table 1 Correlation coefficients for the time series of the wavelet coefficients between GRACE and hydrology.

Wavelet Scale 2	Memphis	Manaus	Monghyr
CPC	0.70	0.93	0.95
LaD	0.17	0.89	0.91

Table 2 Correlation coefficients for the time series of the wavelet coefficients between GRACE and hydrology (see Fig. 17).

Wavelet Scale 3	Memphis	Manaus	Monghyr
CPC	0.70	0.89	0.97
LaD	0.67	0.85	0.90

Table 3 Correlation coefficients for the time series of the wavelet coefficients computed between GRACE and hydrology (see Fig. 18).

Wavelet Scale 4	Memphis	Manaus	Monghyr
CPC	0.75	0.83	0.91
LaD	0.66	0.79	0.77

Finally, we illustrate in Fig. 19 - 22 the dimensionless wavelet variances for scale 3 and 4 in October 2003 and April 2004. Obviously, the wavelet variances characterize the regional energy content in the signal. This is in contrast to the well-known degree variances which do not enable an interpretation of any regional change of energy.

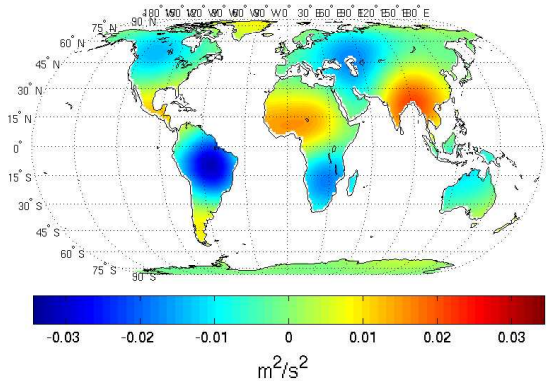

Fig. 5 Anomalies of the gravitational potential observed by GRACE at wavelet scale 3 in October 2003.

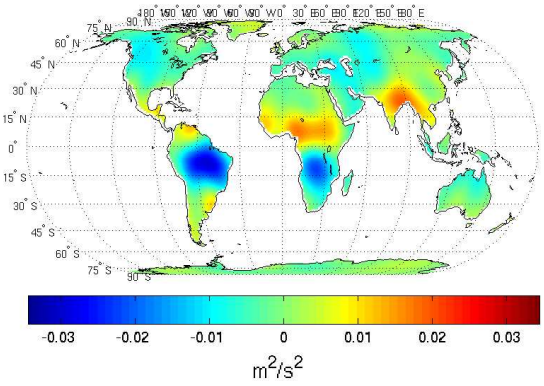

Fig. 6 Anomalies of the gravitational potential observed by GRACE at wavelet scale 4 in October 2003.

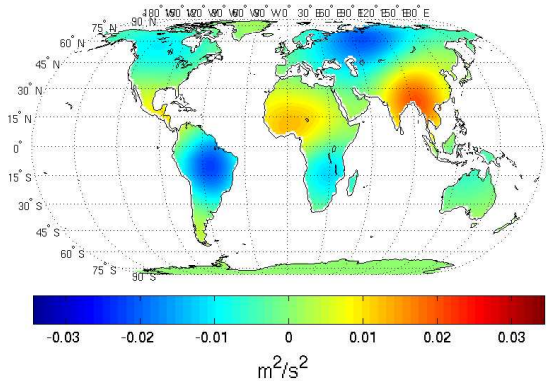

Fig. 7 Anomalies of the gravitational potential computed from LaD model at wavelet scale 3 in October 2003.

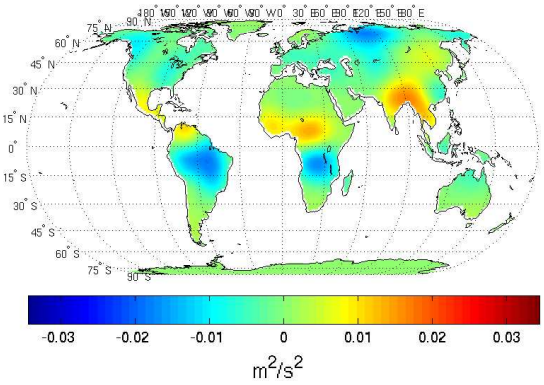

Fig. 8 Anomalies of the gravitational potential computed from LaD model at wavelet scale 4 in October 2003.

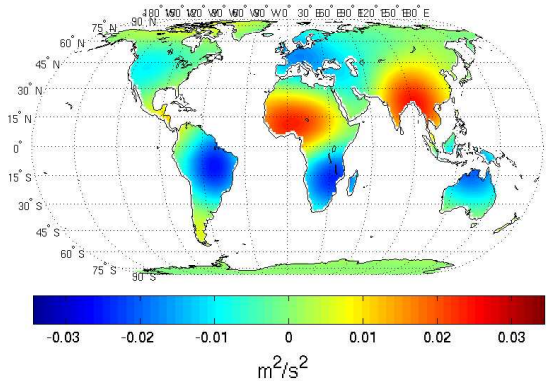

Fig. 9 Anomalies of the gravitational potential computed from CPC model at wavelet scale 3 in October 2003.

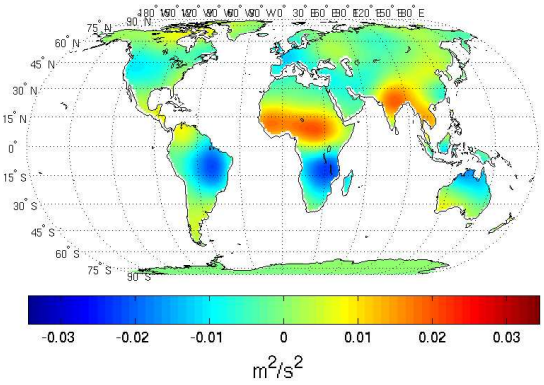

Fig. 10 Anomalies of the gravitational potential computed from CPC model at wavelet scale 4 in October 2003.

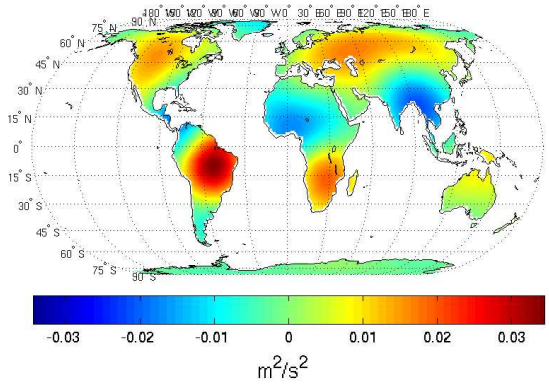

Fig. 11 Anomalies of the gravitational potential observed by GRACE at wavelet scale 3 in April 2004.

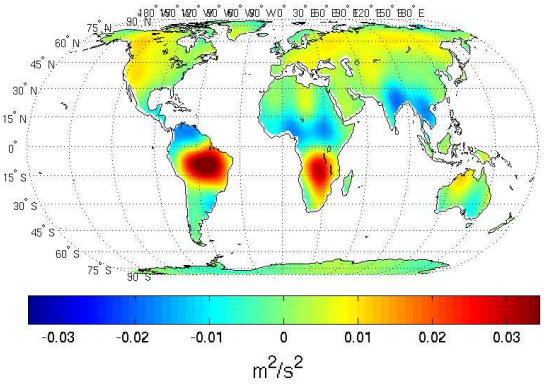

Fig. 12 Anomalies of the gravitational potential observed by GRACE at wavelet scale 4 in April 2004.

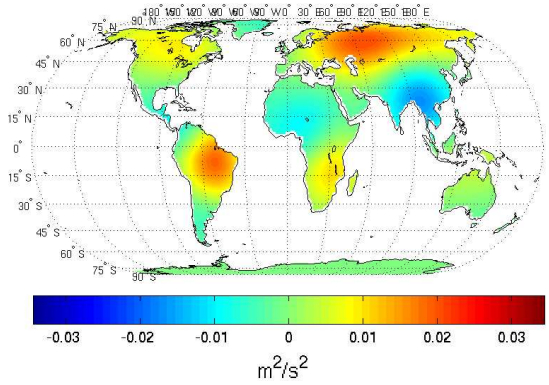

Fig. 13 Anomalies of the gravitational potential computed from LaD model at wavelet scale 3 in April 2004.

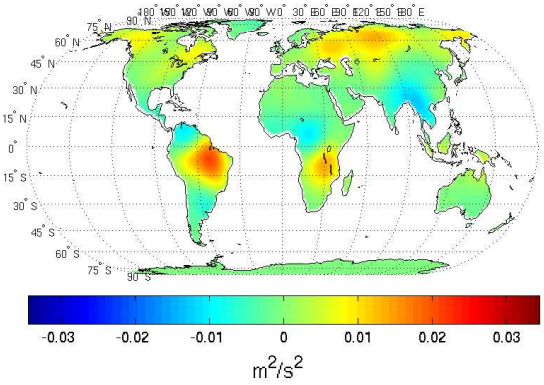

Fig. 14 Anomalies of the gravitational potential computed from LaD model at wavelet scale 4 in April 2004.

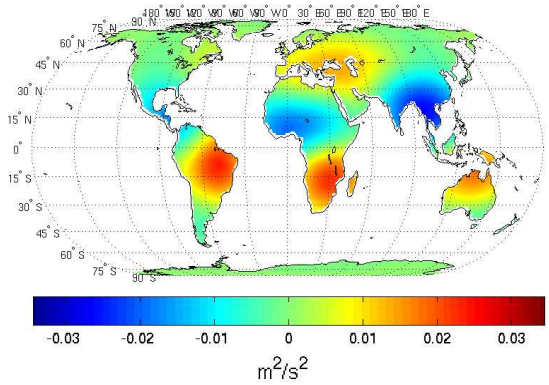

Fig. 15 Anomalies of the gravitational potential computed from CPC model at wavelet scale 3 in April 2004.

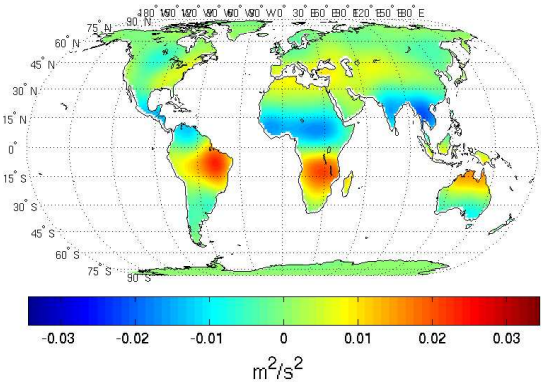

Fig. 16 Anomalies of the gravitational potential computed from CPC model at wavelet scale 4 in April 2004.

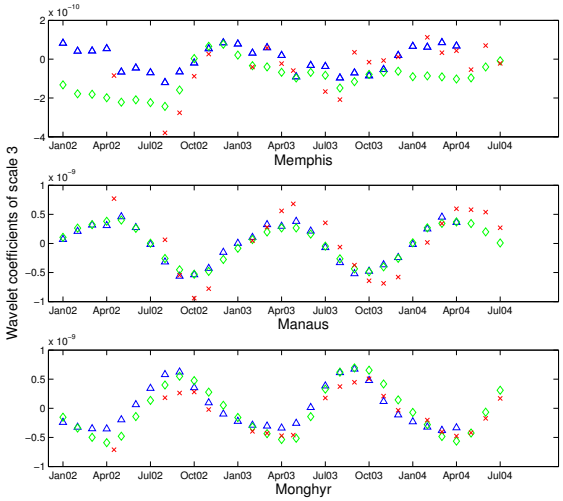

Fig. 17 Time series of wavelet coefficients of scale 3 obtained from GRACE(×), CPC(⋄), LaD(△) at Memphis (Tennessee), Manaus (Brazil), and Monghyr (India) during the months 01/2002-07/2004.

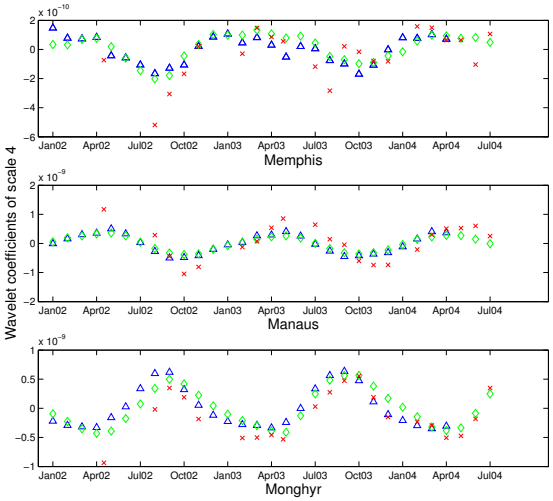

Fig. 18 Time series of wavelet coefficients of scale 4 obtained from GRACE(×), CPC(⋄), LaD(△) at Memphis (Tennessee), Manaus (Brazil), and Monghyr (India) during the months 01/2002-07/2004.

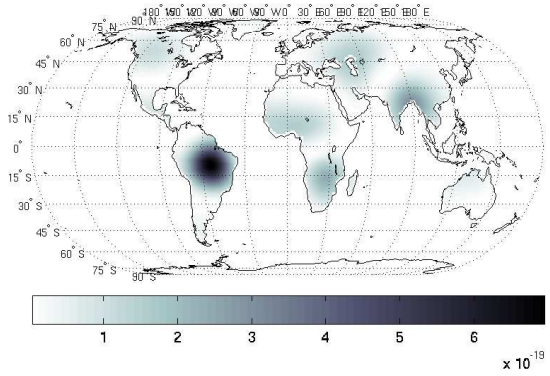

Fig. 19 GRACE wavelet variances of scale 3 in October 2003.

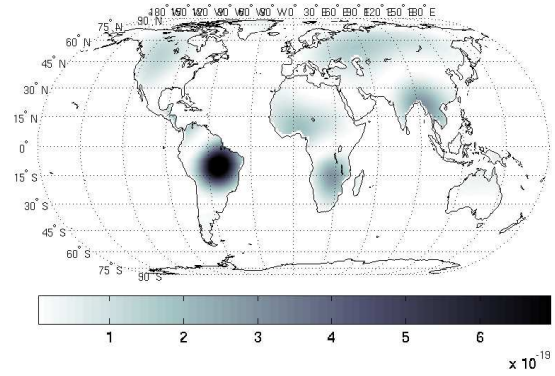

Fig. 20 GRACE wavelet variances of scale 3 in April 2004.

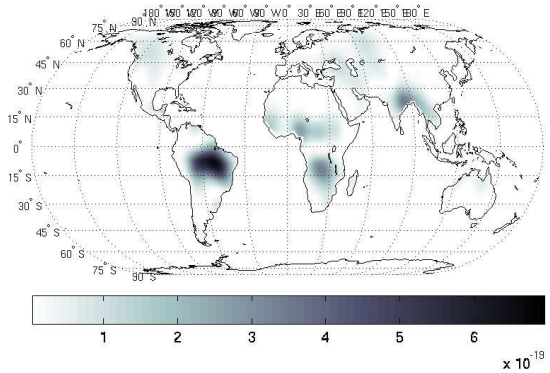

Fig. 21 GRACE wavelet variances of scale 4 in October 2003.

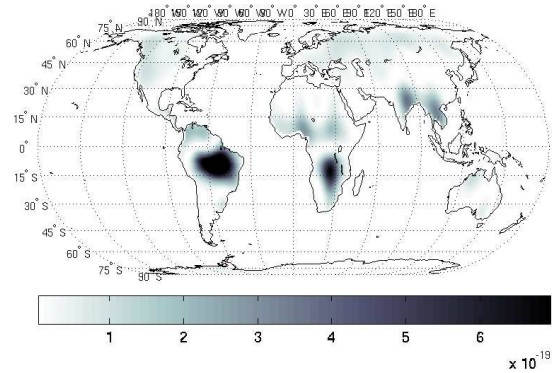

Fig. 22 GRACE wavelet variances of scale 4 in April 2004.

7 Concluding Remarks

In this work we analyze the Earth's gravitational potential observed monthly by GRACE. We compute wavelet expansions of the gravitational field using CuP wavelets. Thereby, we observe seasonal variations in the wavelet coefficients. The wavelet coefficients show strong correlations to the gravitational signal computed from the output of the hydrological models LaD and CPC (see Table 1-3). This correlation also becomes visible in the spatial domain. The wavelet scales 3 and 4 are the most suited scales for this analysis, since they fit best to the spatial extension of the investigated phenomena. The numerical results are similar and in agreement to those obtained in previous studies (see, for example, Wahr et al. (2004); Tapley et al. (2004b)), more details can be found in Kohlhaas (2005). This shows that wavelets are an appropriate tool to investigate regional and temporal variations in the gravitational field.

Since the point of departure in this study are the monthly GRACE gravity fields provided by the GRACE science team, no higher temporal resolution could be obtained. Recent studies showed that starting from the original GRACE observations the temporal resolution of the gravity variations could be increased regionally (Rowlands et al. (2005); Han et al. (2005a,b)) at least by a factor of 2. Consequently, in a next step, it would be of interest to use the proposed wavelets for a direct gravity computation from GRACE observations with the intention of a high temporal and spatial resolution.

Acknowledgements We are thankful to the authors of the hydrology models at the Climate Prediction Center of NOAA and the US Geological Survey (USGS) for providing the hydrology data and to the GRACE science team and CSR-UT for providing the GRACE monthly gravity fields. Moreover, we gratefully acknowledge the financial support by the Forschungsschwerpunkt "Mathematik und Praxis", and the Graduiertenkolleg "Mathematik und Praxis" of the University Kaiserslautern.

References

Andersen OB, Hinderer J (2005) Global Inter-Annual Gravity Changes from GRACE: Early Results. Geophys Res Lett 32, L01402, doi:10.1029/2004GL020948

Bettadpur S(2003) Level-2 Gravity Field Product User Handbook, GRACE 327-734, CSR Publ GR-03-01, Univ of Texas, Austin

Chen JL, Wilson CR, Tapley BD, Ries JC (2004) Low Degree Gravitational Changes from GRACE: Validation and Interpretation. Geophys Res Lett 31, L22607, doi: 10.1029/2004GL021670

Driscoll JR, Healy, DH jr (1994) Computing Fourier Transforms and Convolutions on the 2-sphere. Adv Appl Math 15: 202-250

Edmonds AR (1964) Drehimpulse in der Quantenmechanik. Bibliograph Inst, Mannheim

Fan Y, van den Dool H (2004) Climate Prediction Center Global Monthly Soil Moisture Data Set at 0.5° Resolution for 1948 to Present. J Geophys Res 109, D10102, doi: 10.1029/2003JD004345

Fengler MJ, Freeden W, Gutting M (2004a) Darstellung des Gravitationsfeldes und seiner Funktionale mit Sphärischen Multiskalentechniken. zfv – Zeitschrift für Geodäsie, Geoinformation und Landmanagement 5: 323-334

Fengler MJ, Freeden W, Michel V (2004b) The Kaiserslautern Multiscale Geopotential Model SWITCH-03 from Orbit Perturbations of the Satellite CHAMP and Its Comparison to the Models EGM96, UCPH2002_02_0.5, EIGEN-1s, and EIGEN-2. Geophys J Int 157: 499-514, doi:10.1111/j.1365-246X.2004.02209.x

Fengler MJ (2005) Vector Spherical Harmonic and Vector Wavelet Based Non-Linear Galerkin Schemes for Solving the Incompressible Navier-Stokes Equation on the Sphere. PhD-thesis (submitted), Univ of Kaiserslautern, Dept of Mathematics, Geomathematics Group

Freeden W (1999) Multiscale Modelling of Spaceborne Geodata. BG Teubner, Stuttgart

Freeden W, Maier T (2002) On Multiscale Denoising of Spherical Functions: Basic Theory and Numerical Aspects. ETNA 14:40-62 BG Teubner, Stuttgart

Freeden W, Michel V (2004) Multiscale Potential Theory (With Applications to Earth's Sciences). Birkhäuser Verlag, Berlin

Freeden W, Schreiner M (1995) Non-Orthogonal Expansions on the Sphere. Math Meth in the Appl Sci 18:83-120

Freeden W, Windheuser U (1996) Spherical Wavelet Transform and Its Discretization. Adv Comput Math 5: 51-94

Freeden W, Gervens T, Schreiner M (1998) Constructive Approximation on the Sphere (With Applications to Geomathematics). Oxford Sci Publ, Clarendon

Han SC, Shum CK, Braun A (2005a) High-Resolution Continental Water Storage Recovery from Low-Low Satellite-To-Satellite Tracking. J Geodyn 39: 11-28

Han SC, Shum CK, Jekeli C, Alsdorf D (2005b) Improved Estimation of Terrestrial Water Storage Changes from GRACE. Geophys Res Lett 32, L07302, doi:10.1029/2005GL022382

Jekeli C (1981) Alternative Methods to Smooth the Earth's Gravity Field, Rep 327. Dept Geod Sci & Surv, Ohio State Univ, Columbus

Kohlhaas AC (2005) Multiscale Modelling of Temporal and Spatial Variations in the Earth's Gravity Potential Observed by GRACE, Diploma-thesis, Univ of Kaiserslautern, Dept of Mathematics, Geomathematics Group.

Maier T (2003) Multiscale Geomagnetic Field Modelling from Satellite Data. PhD-thesis, Univ of Kaiserslautern, Dept of Mathematics, Geomathematics Group.

Mayer C (2003) Wavelet Modelling of Ionospheric Currents and Induced Magnetic Fields From Satellite Data. PhD-thesis, Univ of Kaiserslautern, Dept of Mathematics, Geomathematics Group.

Milly PCD, Shmakin AB (2002) Global Modeling of Land Water and Energy Balances. Part I: The Land Dynamics (LaD) Model. J Hydrometeo 3: 283-299

Ramillien G, Cazenave A, Brunau O (2004) Global Time Variations of Hydrological Signals from GRACE Satellite Gravimetry. Geophys J Int 158: 813-826, doi:10.1111/j.1365-264X.2004.02328.x

Rowlands DD, Luthcke SB, Klosko SM, Lemoine FGR, Chinn DS, McCarthy JJ, Cox CM, Andersen OB (2005) Resolving Mass Flux at High Spatial and Temporal Resolution Using GRACE Intersatellite Measurements. Geophys Res Lett 32, L04310 doi:10.1029/2004GL021908

Swenson S, Wahr J (2002) Methods for inferring regional surface-mass anomalies from Gravity Recovery and Climate Experiment measurements of time-variable gravity. J Geophys Res 107(B9), 2193, doi:10.1029/2001JB000576

Swenson S, Wahr J, Milly PCD (2003) Estimated Accuracies of Regional Water Storage Variations inferred from the Gravity Recovery and Climate Experiment (GRACE). Water Resour Res 39(8), 1223, doi:10.1029/2002WR001808

Tapley BD, Bettadpur S, Watkins MM, Reigber C (2004a) The Gravity Recovery and Climate Experiment: Mission Overview and Early Results. Geophys Res Lett 31, L09607, doi:10.1029/2004GL019920

Tapley BD, Bettadpur S, Ries JC, Thompson PF, Watkins MM (2004b) GRACE Measurements of Mass Variability in the Earth System. Science 305: 503-505

Wahr J, Molenaar M, Bryan F (1998) Time Variability of the Earth's Gravity Field: Hydrological and Oceanic Effects and Their Pos-

sible Detection Using GRACE. J Geophys Res 103(B12): 30205-30229

Wahr J, Swenson S, Zlotnicki V, Velicogna I (2004) Time-Variable Gravity from GRACE: First Results. Geophys Res Lett 31, L11501, doi:10.1029/2004GL019779

Folgende Berichte sind erschienen:

2003

Nr. 1 S. Pereverzev, E. Schock.
On the adaptive selection of the parameter in regularization of ill-posed problems

Nr. 2 W. Freeden, M. Schreiner.
Multiresolution Analysis by Spherical Up Functions

Nr. 3 F. Bauer, W. Freeden, M. Schreiner.
A Tree Algorithm for Isotropic Finite Elements on the Sphere

Nr. 4 W. Freeden, V. Michel (eds.)
Multiscale Modeling of CHAMP-Data

Nr. 5 C. Mayer
Wavelet Modelling of the Spherical Inverse Source Problem with Application to Geomagnetism

2004

Nr. 6 M.J. Fengler, W. Freeden, M. Gutting
Darstellung des Gravitationsfeldes und seiner Funktionale mit Multiskalentechniken

Nr. 7 T. Maier
Wavelet-Mie-Representations for Soleniodal Vector Fields with Applications to Ionospheric Geomagnetic Data

Nr. 8 V. Michel
Regularized Multiresolution Recovery of the Mass Density Distribution From Satellite Data of the Earth's Gravitational Field

Nr. 9 W. Freeden, V. Michel
Wavelet Deformation Analysis for Spherical Bodies

Nr. 10 M. Gutting, D. Michel (eds.)
Contributions of the Geomathematics Group, TU Kaiserlautern, to the 2nd International GOCE User Workshop at ESA-ESRIN Frascati, Italy

Nr. 11 M.J. Fengler, W. Freeden
A Nonlinear Galerkin Scheme Involving Vector and Tensor Spherical Harmonics for Solving the Incompressible Navier-Stokes Equation on the Sphere

Nr. 12 W. Freeden, M. Schreiner
Spaceborne Gravitational Field Determination by Means of Locally Supported Wavelets

Nr. 13 F. Bauer, S. Pereverzev
Regularization without Preliminary Knowledge of Smoothness and Error Behavior

Nr. 14 W. Freeden, C. Mayer
Multiscale Solution for the Molodensky Problem on Regular Telluroidal Surfaces

Nr. 15 W. Freeden, K. Hesse
Spline modelling of geostrophic flow: theoretical and algorithmic aspects

2005

Nr. 16 M.J. Fengler, D. Michel, V. Michel
Harmonic Spline-Wavelets on the 3-dimensional Ball and their Application to the Reconstruction of the Earth's Density Distribution

from Gravitational Data at Arbitrarily Shape Satellite Orbits

Nr. 17 F. Bauer
Split Operators for Oblique Boundary Value Problems

Nr. 18 W. Freeden, M. Schreiner
Local Multiscale Modelling of Geoidal Undulations from Deflections of the Vertical

Nr. 19 W. Freeden, D. Michel, V. Michel
Local Multiscale Approximations of Geostrophic Flow: Theoretical Background and Aspects of Scientific Computing

Nr. 20 M.J. Fengler, W. Freeden, M. Gutting
The Spherical Bernstein Wavelet

Nr. 21 M.J. Fengler, W. Freeden, A. Kohlhaas, V. Michel, T. Peters
Wavelet Modelling of Regional and Temporal Variations of the Earth's Gravitational Potential Observed by GRACE

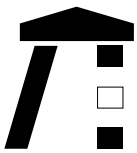

TECHNISCHE UNIVERSITÄT
KAISERSLAUTERN

Informationen:

Prof. Dr. W. Freeden
Prof. Dr. E. Schock
Fachbereich Mathematik
Technische Universität Kaiserslautern
Postfach 3049
D-67653 Kaiserslautern
E-Mail: freeden@mathematik.uni-kl.de
schock@mathematik.uni-kl.de